Nuclear Physics A513 (1990) 636–652
North-Holland

HYPERNUCLEUS FORMATION AFTER ANTIPROTON ANNIHILATION ON NUCLEI

J. CUGNON, P. DENEYE and J. VANDERMEULEN

Université de Liège, Physique Nucléaire Théorique, Institut de Physique au Sart Tilman, Bâtiment B.5, B-4000 Liege 1, Belgium

Received 8 January 1990

Abstract: The hypernucleus formation after antiproton annihilation on atomic nuclei is studied in the frame of an intranuclear cascade picture. The basic mechanism is the formation of an antikaon in the annihilation itself, followed by the production and the capture of a hyperon. The associated production by other mesons is also considered. Comparison with experimental data of the PS177 experiment at LEAR is carried out. It is shown that the excitation of the target by all the cascading particles plays a crucial role for the determination of fraction of the hypernucleus yield which is detectable by the above-mentioned experiment. Our results are roughly consistent with the observed production rates. The kaon-hypernucleus angular correlation pattern is investigated and seems to disagree with recent measurements. The mass residues distribution is also studied. The question of the $B = 1$ annihilations is investigated and is shown that this process could be present with a frequency of less than 20%.

1. Introduction

In the recent PS177 experiment [1-3]) at the LEAR facility, delayed fission with lifetime of the order of 10^{-10} s were observed after antiproton annihilation on Bi and U nuclei. According to the authors of the experiment, the observed delayed fission corresponds to the decay of a hypernucleus formed as a result of the annihilation. The latter can indeed provide the necessary strangeness for this to be possible. This explanation is the most satisfactory one up to now. Alternative explanations (like isomeric states, ...) are on even more shaky ground [3]).

In recent years, emphasis has been put on strangeness production in antiproton annihilation on nuclei, since it could indicate the formation of a supercooled quark-gluon plasma [4]) or the direct annihilation on two or more nucleons [5]) (the so-called $B \geq 1$ annihilations). Even though the basic physics underlying these two possible new phenomena are quite different, an enhanced strangeness production is predicted in both cases. Few experiments testing these ideas have been done so far. Detailed analyses [6-8]) of the KEK experiment [9]), of the LEAR streamer chamber experiment [10]) and of the older Condo experiment [11]) seem to indicate that data are consistent with a conventional picture of the annihilation on a *single* nucleon followed by a rescattering process, in spite of the fact that problems are still pending. The seemingly enhanced Λ production can be explained by a detailed description of the rescattering process, where the strangeness exchange plays a crucial role [7]).

0375-9474/90/$03.50

In this paper we want to examine the case of the only other experiment dealing with strangeness production following antiproton annihilation on nuclei, if one excepts deuteron targets (of which we will say a few words in sect. 8). In sect. 2, we discuss the basic mechanisms leading to delayed fission. In sect. 3, we explain our model based on the intranuclear cascade picture. In sect. 4, we present our results for the hypernucleus yield, assuming the conventional picture. Sect. 5 is devoted to the discussion of the accuracy of our results. Further results on the mass distribution and correlations are discussed in sect. 6. Sect. 7 deals with the possible $B=1$ annihilations. Finally, sect. 8 contains a discussion of our results and a conclusion.

2. Mechanisms leading to delayed fission

According to ref. [1]), the delayed fission with lifetime of the order of 10^{-10} s can originate from the following sequence of reactions

$$\bar{\mathrm{N}}\mathrm{N} \rightarrow \bar{\mathrm{K}}\mathrm{K}l\pi\,, \tag{2.1}$$

$$\bar{\mathrm{K}} + (A-1) \rightarrow {}_{\Lambda}(A-1) + \pi\,, \tag{2.2}$$

followed by hyperon decay, which mainly proceeds by

$$\Lambda\mathrm{N} \rightarrow \mathrm{NN}\,, \tag{2.3}$$

triggering hypernucleus fission. This mechanism is not the only possible one (see below). Step (2.3) may deliver up to 170 MeV to the hypernucleus. For a hyper-U-like nucleus, this is expected to lead to fission in any case, but a hyper-Bi-like nucleus still has a great chance to dissipate this excitation energy by other channels. This is expectedly responsible for the large difference observed in the yields [12]) for U and Bi targets: $(6.5\pm2)\times10^{-4}$ delayed fission per annihilation in uranium and $(2\pm0.6)\times10^{-4}$ in bismuth. Therefore, the *hypernucleus formation yield* H can be rather safely considered as given by the same figure $(6.5\pm2)\times10^{-4}$ for uranium. For the bismuth case, the situation is rather imprecise. In ref. [12]), it is quoted that H may be substantially larger than the delayed fission yield and lie between 8×10^{-4} and 4×10^{-3}. This uncertainty is due to the poor knowledge of the fissibility of an excited nucleus when the excitation energy is high and the fissility parameter is low, although this problem has been discussed in recent times [13-16]). We will disregard this aspect here and concentrate on the quantities H as given in ref. [12]).

The description of the mechanism leading to hypernucleus via (2.1) and (2.2) should be refined. First, the fate of the accompanying pions in (2.1) and the effects of secondaries should be studied since they may excite the target prior to or after Λ-fixation and so lead to prompt fission, which will escape detection in the experimental set up of refs. [1,2]). Even for Bi, this aspect is not negligible since the excitation of the target may reach several hundreds of MeV; it will be detailed in the next section.

Still working in the frame of $B=0$ annihilations, one has to account for other channels than the process in (2.1) and (2.2). The most important ones are the formation of the Σ hypernuclei and the associated production initiated by ω-mesons issued from the annihilation. We will detail these processes below.

3. Our model

3.1. BASIC FEATURES

The stopped antiproton is assumed to annihilate from a Coulomb state and give rise to mesons: pions, kaons, antikaons and ω mesons with the abundances observed in the antinucleon-nucleon annihilations. The subsequent reinteractions of all the particles are followed by means of an intranuclear cascade (INC) model which is basically the same as in ref. [7]). Some details, particularly important for our purpose here, are recalled below. We record all the events leading to hypernucleus formation and for each of them, the corresponding excitation energy E^* of the target after the cascade process is over. If this energy is too large, according to some criterion to be defined below, the nucleus is assumed to undergo prompt fission. Therefore, we are able to calculate the hypernucleus yield, i.e. the number of hypernuclei which will survive until the hyperon decay.

3.2. DETAILS OF THE CALCULATION

(a) Annihilation. The antiproton is assumed to annihilate from a pure Coulomb $(n, l=n-1)$ state. The value of n is taken from ref. [17]). The momenta of the particles emitted in process (2.1) are taken from a uniform-phase-space distribution and their multiplicity is generated in accordance with the antinucleon-nucleon experimental data.

(b) The cascade. All primordial and secondary particles are followed with the standard procedure of the INC model. The following reactions are considered

$$\pi N \to \pi N, \quad \pi NN \to NN, \tag{3.1}$$

$$KN \to KN, \quad \bar{K}N \to \bar{K}N, \quad \bar{K}N \to \Lambda\pi, \quad \bar{K}N \to \Sigma\pi, \tag{3.2}$$

$$\Lambda N \to \Lambda N, \quad \Lambda N \leftrightarrow \Sigma N, \quad \Sigma N \to \Sigma N. \tag{3.3}$$

The detail of the description of the cross-sections and of the angular distributions is given in ref. [7]). We also include Pauli correcting factors in order to cope with the exclusion principle. The Fermi motion of the struck nucleon is taken into account.

(*c*) *The hypernucleus formation.* All baryons are assumed to move in potential wells and to be reflected on or transmitted through the potential wall according to their energy [see refs. [7,18]) for detail]. The depth of the nucleon potential well is taken to be 40 MeV. For Λ-particles, the depth is chosen as 30 MeV, which is a

reasonable number for heavy nuclei, according to ref. [19]). For Σ-particles, we also used 30 MeV, in analogy with Λ-particles (see sect. 7, however). We use the criterion that a hypernucleus is created whenever the hyperon is reflected by the nuclear surface. We furthermore look at the excitation energy of the *hypernuclear residue* E^* (at the end of the cascade) as defined by

$$E^* = K_{\rm res} - \left(\frac{A_{\rm N}}{A_{\rm T}-1}\right)^{5/3} K_T^0 + K_{\rm Y} - K_{\rm Y}^{\rm s}, \tag{3.4}$$

where $K_{\rm res}$ is the kinetic energy of the nucleons in the residue, $A_{\rm N}$ the number of these nucleons, $A_{\rm T}$ the target mass number, $K_{\rm T}^0$ the Fermi motion energy in the target ground state, $K_{\rm Y}$ the kinetic energy of the hyperon and $K_{\rm Y}^{\rm s}$ its value for the lowest possible orbital. Formula (3.4) relies on the Fermi gas picture underlying the INC model and neglects rearrangement energy. This is quite reasonable when the depopulation of the target is small. We make the hypothesis that prompt fission will occur whenever $E^* > E_{\rm PF}$. The quantity $E_{\rm PF}$ should be viewed as an *ad hoc* parameter. Its value will be discussed below. We thus consider hypernuclei with a hyperon on any bound orbit and any particle-hole states for the nucleons provided the overall excitation is lower than $E_{\rm PF}$.

Note that if the $\bar{\rm K}$ produces first a Λ-particle, the residue can ultimately be a Σ-hypernucleus and *vice versa*, owing to the strangeness exchange reactions $\Lambda {\rm N} \leftrightarrow \Sigma {\rm N}$. Since the experiment does not distinguish between Λ- and Σ-hypernucleus, both are included in the quantity H.

(*d*) *ω-induced hypernucleus formation.* Along the same lines, we also include the following possibilities:

$$ {\rm N}\bar{\rm N} \rightarrow \omega + m\pi , \tag{3.5a}$$

$$ \omega {\rm N} \rightarrow {\rm YK} , \quad {\rm Y} = \Sigma, \Lambda \tag{3.5b}$$

with the same possibilities for the hyperon as above. The energy spectra of the ω's and of the accompanying particles are constructed as follows. We have introduced in the statistical model of ref. [20]) the long-lived resonances ω and η, adapting the interaction volume to keep the final pion multiplicity (after ω, η decay) constant. The predicted rates are compatible with experiment. The most frequent pion multiplicities associated to ω are 2 and 3, with $\langle m \rangle = 2.51$. The production of Λ by η is quite negligible for annihilation at rest. The ω production rate is taken to be 0.28, according to refs. [21,22]).

3.3. GENERAL FORMULAE

In order to make the discussion of the results more transparent we can write down the hypernucleus yield H_0 (in $B = 0$ annihilations) in the form

$$H_0 = \sum_{{\rm m}=\bar{\rm K},\omega} \sum_{{\rm Y}=\Sigma,\Lambda} H_0({\rm m}, {\rm Y}) , \tag{3.6a}$$

with, according to the model described in sect. 3.2

$$H_0(\mathrm{m}, \mathrm{Y}) = \mathrm{Prob}\,(\{\mathrm{m\ is\ produced}\} \cap \{\mathrm{m\ interacts}\} \cap \{\mathrm{mN} \to \mathrm{Ym'\ occurs}\} \cap \{\mathrm{Y\ is\ fixed}\} \cap \{E^* < E_{\mathrm{PF}}\})\,, \tag{3.6b}$$

where in fact the successive classes of events form a hierarchy (m′ stands for π or K when $\mathrm{m} = \bar{\mathrm{K}}$ or ω, respectively). A given class is totally contained in the preceding one. Therefore, one can write, in terms of conditional probabilities [23]):

$$H_0(\mathrm{m}, \mathrm{Y}) = P(\mathrm{A})P(\mathrm{B}|\mathrm{A})P(\mathrm{C}|\mathrm{B})P(\mathrm{D}|\mathrm{C})P(\mathrm{E}|\mathrm{D})\,, \tag{3.7a}$$

where A, . . . , E represent the hierarchy of classes in eq. (3.6b). With more transparent notation, we rewrite expression (3.7a) as

$$H_0(\mathrm{m}, \mathrm{Y}) = P_{\mathrm{m}} P_{\mathrm{int}}^{(\mathrm{m})} \sum_{\mathrm{Y'}=\Sigma,\Lambda} P(\mathrm{mN} \to \mathrm{Y'm'}) P_{\mathrm{f}}(\mathrm{Y'}, \mathrm{Y}) P(E^* < E_{\mathrm{PF}})\,, \tag{3.7b}$$

where P_{m} is the branching ratio for meson m in the annihilation, $P_{\mathrm{int}}^{(\mathrm{m})}$ is the probability for this meson m to interact, $P(\mathrm{mN} \to \mathrm{Y'm'})$ is the probability for the indicated reaction to occur, $P_{\mathrm{f}}(\mathrm{Y'}, \mathrm{Y})$ is the probability that the formation of a hyperon Y′ ultimately leads to the fixation of a hyperon Y. The last factor is the probability of having a sufficiently low excitation energy.

4. Numerical results

4.1. GLOBAL YIELDS

The only somewhat uncertain parameter in our approach is the quantity E_{PF} (eq. (3.7b)). One can try to determine its value from experimental data concerning the energy dependence of the fissility and tentatively chose it as the value of the excitation energy at which the ratio $\Gamma_{\mathrm{n}}/\Gamma_{\mathrm{f}}$ (of the average neutron and fission widths) is roughly equal to unity. Unfortunately, experimental data are scarce and not very precise [24]). We deduce from refs. [24-26]) that $E_{\mathrm{PF}} \approx 50$ MeV for Bi and ≈ 15 MeV for U. The different values obviously come from the different fissilities. (Note that $\Gamma_{\mathrm{n}}/\Gamma_{\mathrm{f}}$ is slowly varying with E^* for U due to the approximate equality between the fission barrier and the neutron separation energy). In any case, we give below in table 1 results for different values of E_{PF} in order to estimate upper and lower bounds. The global hypernucleus yield is quite comparable with experiment. Several remarks are however in order. First, the yield for Bi is about four times as large as for U. This is a direct consequence of fissility. Second, Σ-hypernuclei are produced much less abundantly than Λ-hypernuclei, but neglecting Σ-Λ interchange would reverse this relative importance and also enhance the total yield by about a factor of 2. The explanation is the following: Σ's are transformed easily into Λ's through the $\Sigma\mathrm{N} \to \Lambda\mathrm{N}$ reaction and give then rapidly moving Λ's which have a small chance to be fixed. Third, the ω-contribution is two times smaller than the $\bar{\mathrm{K}}$ one.

4.2. INTERMEDIATE RESULTS

Let us concentrate on a single contribution, say $H_0(\bar{K}, \Lambda)$ for simplicity. We will detail the different factors appearing in eq. (3.7). We start with discussing simple estimates for each of them. The quantity P_m is taken equal to 0.05. In first approximation, $P_{int}^{(m)} \approx \Omega/4\pi$, where Ω is the average solid angle under which the nucleus is seen from the annihilation site, leading to $P_{int}^{(m)} \approx 0.3$ for U. The next factor may be roughly evaluated by $P(\bar{K}N \to Y\pi) \approx 1 - \exp(-\sigma(\bar{K}N \to Y\pi)\rho\langle d\rangle)$ where $\langle d\rangle$ is the average length of the $\bar{K}$ trajectory inside the nucleus. With $\sigma(\bar{K}N \to \Lambda\pi) \approx 3.7$ mb, $\sigma(\bar{K}N \to \Sigma\pi) \approx 7.5$ mb which are typical values for the average $\bar{K}$ momentum, and standard values for the nuclear parameters, one has $P(\bar{K}N \to Y\pi) \approx 0.8$. The quantity $P_f(Y, \Lambda)$ is not easy to evaluate so simply. It roughly corresponds to the fraction of the produced Λ's which are "slow enough". This of course depends upon the spectrum of the primordial $\bar{K}$'s and upon the kinematics (see fig. 1). As underlined in several references [1,2,27]), the spectrum of the $\bar{K}$'s shows a peak around the "magic" kinematics [28]). On this basis, one expects $P_f(\Sigma, \Lambda) + P_f(\Lambda, \Lambda) \approx 0.4$, demanding that the Λ is produced with a momentum less than, say ~ 150 MeV/c. This is probably a rough estimate, since one has to take into account the Σ's which are formed through $\bar{K}N \to \Sigma\pi$ reactions and subsequent transformation of Σ's into Λ's and also

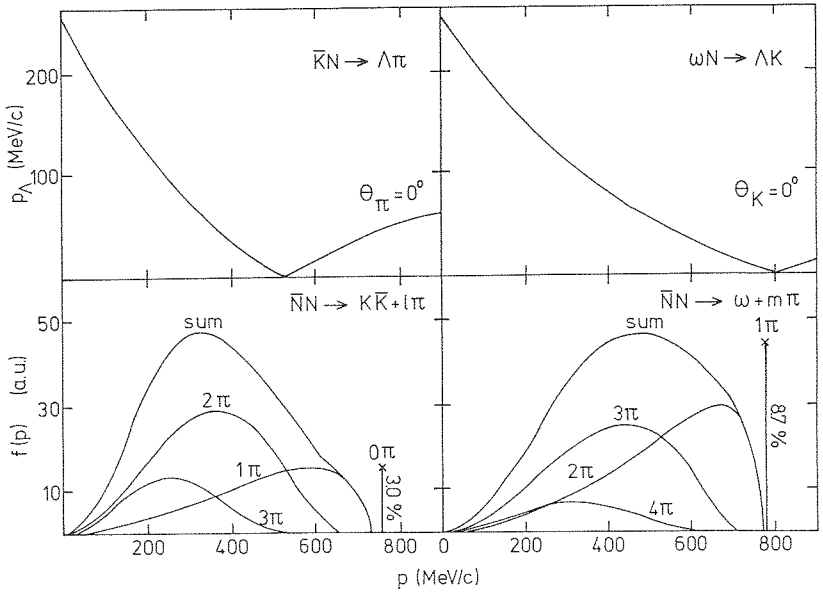

Fig. 1. *The lower parts* show the $\bar{K}$ (left) and ω (right) momentum spectra for various annihilation channels in $\bar{N}N$ system, as evaluated by a uniform-phase-space model. The absolute normalisation of the various components is proportional to the corresponding branching ratios as estimated by the statistical model of ref. [20]). *The upper parts* of the figure give the momentum of the hyperon produced in the indicated processes as a function of the momentum of the incident $\bar{K}$ (left) or ω (right), exhibiting the so-called magic kinematics [28]), when the final meson is produced forward.

the Λ's which are produced with higher momentum and which are sufficiently slowed down (see fig. 2). The last factor in eq. (3.7) stands for discarding too much excited nuclei, which would decay by prompt fission and so escape from detection in the PS177 experiment apparatus. The excitation energy depends upon the dynamical story of the primordial pions, of the K and $\bar{\mathrm{K}}$ mesons and of the hyperon after its formation. We would like to stress that the evaluation of this factor and, to a lesser extent, of $P_{\mathrm{f}}(\mathrm{Y}, \mathrm{Y})$, requires the complexity of the full cascade process. Our calculation provides the best estimate for this factor.

The spectrum of the hypernucleus excitation energy E^* when the cascade is over is depicted in fig. 3. We emphasize that E^* is different from the energy E_{tr} delivered by the annihilation products (see fig. 4), the remaining part being carried away by fast (nucleon, pion) particles. The steep rise near 400 MeV in the distribution of E_{tr} comes from the absorption of one pion. The average value of $E^*(\approx 100\,\mathrm{MeV})$ is about half the value quoted in ref. [29]) for all events. This is not surprising since hypernucleus formation is expected to occur in rather "soft" events only. Looking at fig. 2, one has $P(\mathrm{E}^* < E_{\mathrm{PF}}) \approx 0.05$ for U and ≈ 0.15 for Bi (in fig. 2, only the spectrum for U is shown, but the one for Bi is roughly the same) with the values of E_{PF} quoted in sect. 4.1. If we gather all the estimated factors, one finds $H_0(\bar{\mathrm{K}}, \Lambda) \approx 2.4 \times 10^{-4}$, very close to the value yielded by the exact calculation. For the sake of

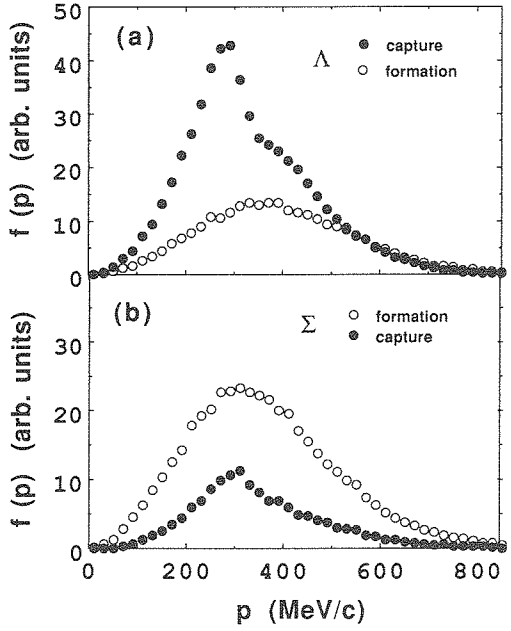

Fig. 2. Comparison between the hyperon (Λ in the upper part, Σ in the lower part) momentum distribution when they are formed (open symbols) and when they are captured (full dots), as calculated in the INC model, for the case of antiproton annihilation at rest on ^{238}U nuclei. In each part, the distribution integrals are proportional to the corresponding multiplicities.

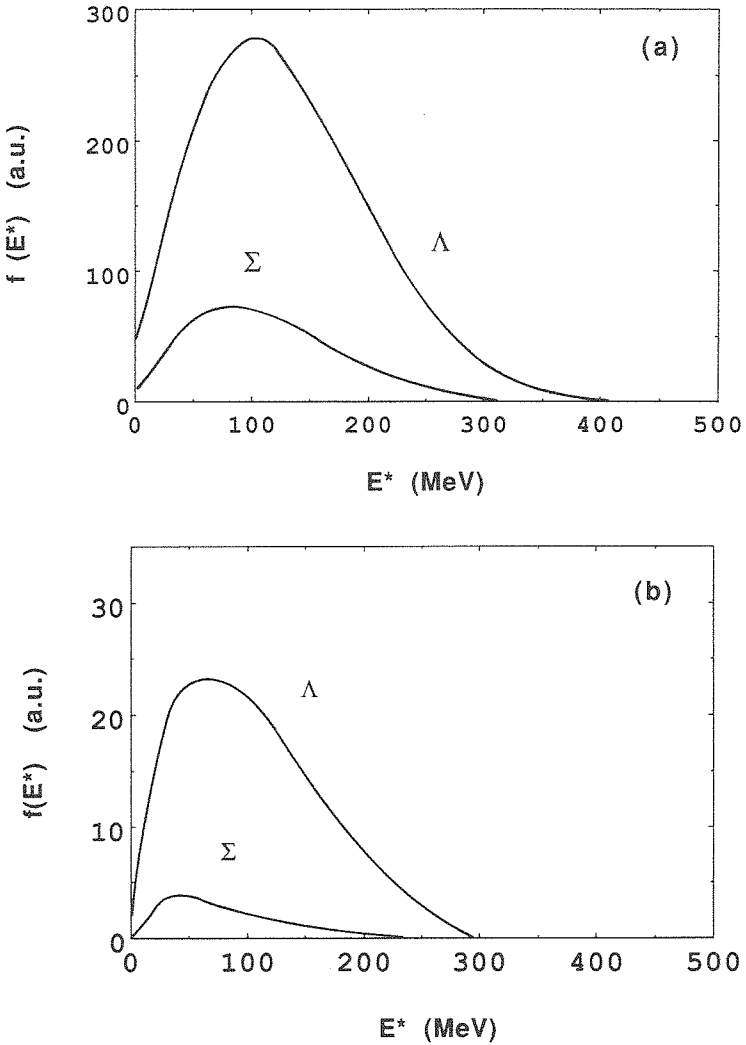

Fig. 3. Distribution of the hypernuclear fragment excitation energy E^* at the end of the cascade process in events where a $\bar{K}$ (a) or a ω (b) is produced in the annihilation. The normalization convention and system are the same as in fig. 2.

comparison, the factors entering eqs. (3.7) obtained in the exact calculation are, for the U case, 0.05, 0.381, 0.90, 0.38 and 0.0475, respectively.

We want to point out the relative importance of the accompanying pions (and kaons) in the cut-off factor on the excitation energy. Roughly speaking, no excitation energy is deposited by these particles, if they miss the nucleus. The corresponding probability p may then be written as

$$p \approx (1 - \Omega/4\pi)^{\langle l \rangle + 1},$$

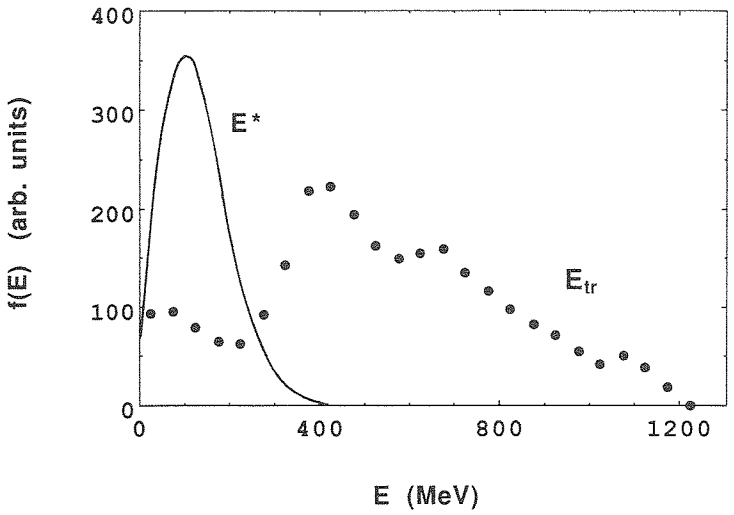

Fig. 4. Comparison between the distribution of the energy E_{tr} transferred to the baryonic system (dots) and the excitation energy E^* left at the end of the cascade (full curve). The system is the same as in fig. 2.

where Ω is the solid angle previously defined and $\langle l \rangle$ is the average pion multiplicity. The latter being ≈ 2, $p \approx 0.25$. Comparing to $P(E^* < E_{PF})$ above convincingly shows that the energy excitation brought in by the $\bar{K}$'s and the subsequent particles are important.

For events initiated by the ω's, $P_m = 0.28$ and $P_{int}^{(\omega)}$ is roughly the same as for $\bar{K}$'s. Comparing to $\bar{K}$'s, the larger value of P_m is roughly compensated by the third factor of eq. (3.7b), which depends upon the cross section. The latter is about five times smaller than in the $\bar{K}$ case. The overall smaller yield for ω-events comes from $P_f(Y, Y)$. The "magic" kinematics is somehow less favorable in the ω-case (see fig. 1).

5. Assessment of the results

5.1. THE ANNIHILATION STATE

We used Coulomb wavefunctions with $n = 9$, following ref. [17]). However, this value is not completely certified and it is possible that several states are involved. We checked that modifying n by one or two units does not bring large changes. For a more inner state (n smaller), the probability that the $\bar{K}$ interacts is larger, but this is compensated by the fact that accompanying pions have then more chance to deposit excitation energy.

5.2. $\bar{K}$ PROPERTIES

The $\bar{K}$ abundance in the annihilation is not precidely known. It lies between 0.04 and 0.06 (see refs. [30,31])). We chose here the average value of 0.05. In ref. [32]), the value 0.06 is used. So, our final results are to be taken at a 10–20% level confidence as far as this point is concerned. If a better measurement of this abundance appeared, our result could be sharpened correlatively. The cross sections for $\bar{K}$ reactions in the momentum range under consideration are rather well known and do not introduce significant uncertainty.

5.3. FIXATION PROBABILITY

We here used a completely classical picture for this process. This may appear as a weak point, since the Λ-capture involves the quantum aspects of the Λ-bound states. However, one has to realize that summation is made over several Λ-bound states (from the bottom to the top of a 30 MeV potential well). Furthermore, the whole spectrum of the $\bar{K}$'s is used. So quantum aspects are presumably washed out to a large extent. They have been studied by Bandō and Žofka [32]). We want to compare our results with their approach.

What is actually calculated in ref. [32]) is the hypernucleus formation probability by a monochromatic parallel $\bar{K}$ beam of 400 MeV/c. The interaction vertex is described classically in terms of the $\bar{K}N \to \Lambda\pi$ cross section, as in our work, but the summation of the quantum overlap between the initial ground state and various Λ-particle–N-hole final states is kept. Furthermore, distorted waves (by complex potentials) both for the incoming antikaon and for the outgoing pion are introduced. The latter point is important. It roughly corresponds to demanding that the antikaon does not interact before making an hyperon and that the outgoing pion does not interact. This procedure more or less corresponds to limiting the excitation energy delivered by these particles. The formation probability is indeed reduced by about a factor 20, in comparison to that obtained by using plane waves instead of distorted waves [33]). As for the final states, all Λ orbitals from 1s up to $3p_{1/2}$ and all nucleon orbitals up to the Fermi level, with $n \leqslant 3$ are introduced. This corresponds to summing states up to a high excitation energy ($\approx$70 MeV), but retaining one-particle–one-hole states only. We suspect that this is roughly equivalent to selecting all states with a rather smaller excitation energy. It is therefore difficult to compare the two approaches. We actually calculated in our model the hypernucleus formation probability by an incoming $\bar{K}$ beam. We obtained a formation probability of 1.0×10^{-2} compared to 2.4×10^{-2} obtained in ref. [32]). It is very hard to disentangle the effects which are contained in our quantity $P(E^* < E_{PF})$ and which are not contained in the quantity N_{eff} of ref. [32]) and *vice versa*. In conclusion, we can only record that our classical method is semi-quantitatively equivalent to the quantum mechanical calculation of ref. [32]) as far as the hypernucleus formation by $\bar{K}$-induced hyperon production with rescattering is concerned.

TABLE 1

Theoretical predictions for partial hypernucleus formation yields $H_0(m, Y)$ (see eqs. (3.6)) and for the total yield H_0 per antiproton annihilation (at rest) on the indicated targets

	^{209}Bi			^{238}U		
	$E_{PF}=40$	$E_{PF}=50$	$E_{PF}=60$	$E_{PF}=10$	$E_{PF}=15$	$E_{PF}=20$
$H_0(\bar{K}, \Lambda)$	5.18	6.96	8.92	1.22	1.73	2.33
$H_0(\bar{K}, \Sigma)$	1.61	2.17	2.83	0.41	0.55	0.71
$H_0(\omega, \Lambda)$	3.35	4.45	5.91	0.49	0.78	1.16
$H_0(\omega, \Sigma)$	0.46	0.68	0.81	0.027	0.05	0.11
$H_0(\bar{K}, \Lambda+\Sigma)$	6.79	9.13	11.75	1.63	2.28	3.04
$H_0(\omega, \Lambda+\Sigma)$	3.81	5.13	6.72	0.52	0.83	1.27
sum $= H_0$	10.62	14.26	18.47	2.15	3.11	4.31

Statistical errors on the calculation are generally around 5%. E_{PF} is given in MeV, yields in 10^{-4}.

5.4. PROMPT FISSION PROBABILITY

This point is rather complex and brings the largest uncertainty. A complete calculation involving the time-dependent competition between evaporation and fission is beyond the scope of this paper. Let us mention that such a calculation would require data in a whole range of excitation energy, which are far from being reliable and complete. Furthermore, it may well happen that the presence of a Λ particle may change quite significantly the fissility. This interesting point has not been investigated so far, to the best of our knowledge Table 1 shows that this aspect of our calculation (and of any other one) makes present predictions not more accurate than a factor 1.5–2 in our opinion.

6. Further results

6.1. THE HYPERNUCLEUS MASS DISTRIBUTION

This quantity, as predicted by our model, is shown in fig. 5. The hypernuclear residue may have a total baryon number $A(=A_N+1)$ down to about fifteen units smaller than the target one, with a small probability however. On the average, the difference amounts to three units. The mass distribution may still be distorted (by neutron evaporation) before the hypernucleus decays by delayed fission. Fig. 5 shows that the lifetimes mentioned in ref. [3]) should be considered as an average value for several hypernuclei with slightly different masses.

6.2. CORRELATIONS

It has been stressed [12]) that the hypernuclear origin of the delayed fission could be certified by detecting a kaon in coincidence with the delayed fission. A recent

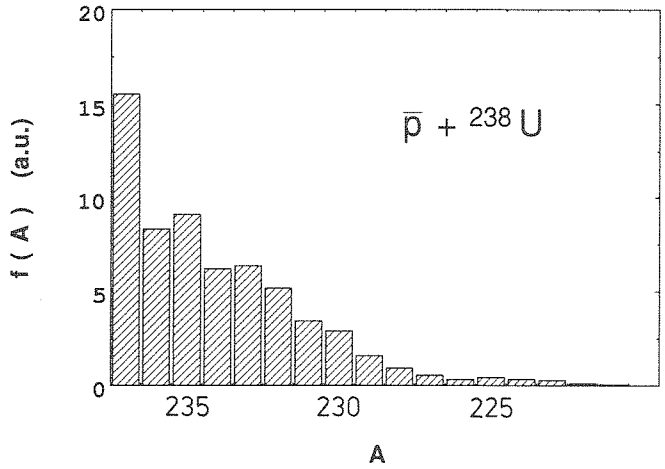

Fig. 5. Distribution of the hypernucleus mass number A after antiproton annihilation on a ^{238}U target.

experiment [34]) has been performed in this perspective (see ref. [12])), which adds to the PS177 apparatus a kaon range telescope placed parallel to the beam downward. With the geometrical arrangement, the efficiency and the counting rates for delayed fission, 6 K^+'s were expected in coincidence assuming isotropic K^+ emission. None was observed. In our model, we calculated the correlation between the direction of the emitted K^+ and the direction of the recoiling hypernucleus. Fig. 6 shows the distribution of the angle θ between the two directions. Emission of the accompanying pions and of fast particles (see fig. 7) is responsible for the partial decorrelation between the direction of strangeness and antistrangeness. Fig. 6 shows a relative depletion of the K^+ yield when the latter is emitted in the same direction as the hypernucleus. This is precisely the geometry adopted in ref. [34]). Therefore, the expectation for the K^+ yield should be reduced from 6 to 4. Therefore the negative result of this experiment is still consistent with the hypernuclear hypothesis, but at the confidence level of 2% only!

7. Two nucleon annihilations

If $B = 1$ annihilations exist, a new possibility for producing hypernuclei is open [20]), namely

$$\bar{p}NN \rightarrow YK + X, \tag{7.1}$$

followed by the fixation of the hyperon. Let us call, in analogy with eqs. (3.6), H_1 the hypernucleus yield for this kind of annihilation. One has

$$H_1 = H_1^{m} + H_1^{B}, \tag{7.2}$$

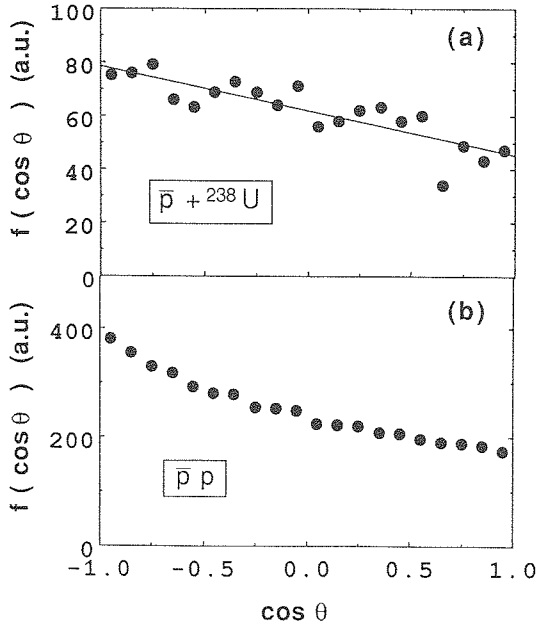

Fig. 6. *Upper part*: distribution of the angle θ between the direction of the emitted kaon and the direction of the recoiling hypernucleus in $B = 0$ annihilations including a $K\bar{K}$ pair (same system as in fig. 2). *Lower part:* distribution of the angle θ between the direction of the emitted kaon and the direction of the antikaon in the primordial $\bar{p}p$ system.

with

$$H_1^{\mathrm{m}} = \sum_{\mathrm{m}=\omega,\bar{K}} \sum_{Y=\Lambda,\Sigma} H_1(\mathrm{m}, Y)\,, \tag{7.3}$$

$$H_1^{\mathrm{B}} = \sum_{Y',Y=\Lambda,\Sigma} H_1(Y', Y)\,. \tag{7.4}$$

The quantity H_1^{m} accounts for the non-hyperonic annihilation channels ($\bar{p}NN \to NK\bar{K}X$) and is similar to H_0 (eqs. (3.6)). The quantity H_1^{B} corresponds to the creation of a hyperon Y′ in the annihilation channel ($\bar{p}NN \to Y'KX$) and to the ultimate formation of a Y-hypernucleus. Similarly to eqs. (3.7) one can write

$$H_1(Y', Y) = P(Y')P_{\mathrm{f}}(Y', Y)P(E^* < E_{\mathrm{PF}})\,, \tag{7.5}$$

where $P(Y')$ is the branching ratio for the appearance of Y′ in $B = 1$ annihilation. All the input data necessary to the calculation are taken from ref. [20]).

The partial yields $H_1(Y', Y)$, as calculated in our model, are given in table 2. They are definitely larger than the H_0 yields, mainly because the hyperon is produced

TABLE 2

Theoretical predictions for partial hypernucleus formation yields $H_I(Y', Y)$ (see eqs. (7.2)) and for the total yield H_I^B per $B=1$ antiproton annihilation (at rest) on the indicated targets

	^{209}Bi			^{238}U		
	$E_{PF}=40$	$E_{PF}=50$	$E_{PF}=60$	$E_{PF}=10$	$E_{PF}=15$	$E_{PF}=20$
$H_I(\Lambda, \Lambda)$	33.85	40.45	47.39	6.35	9.88	14.23
$H_I(\Lambda, \Sigma)$	0	0	0	0	0	0
$H_I(\Sigma, \Lambda)$	9.40	13.56	18.40	2.28	2.99	3.83
$H_I(\Sigma, \Sigma)$	42.79	48.76	54.95	6.61	10.89	16.10
$H_I(\Lambda, \Lambda+\Sigma)$	33.85	40.45	47.39	6.35	9.88	14.25
$H_I(\Sigma, \Lambda+\Sigma)$	52.19	62.32	73.35	8.89	13.88	19.93
sum $=H_I^B$	86.04	102.77	120.74	15.24	23.76	34.16
H_I^m	2.06	2.96	4.27	0.66	0.99	1.18
H_I	88.10	105.73	125.01	15.90	24.75	35.34

Statistical errors are generally around 5%. E_{PF} is given in MeV, yields in 10^{-4}.

directly, with a substantial yield [20]). This is partially compensated by a rather low fixation probability, due to the fact that the hyperons are fairly energetic, with an average kinetic energy around 120 MeV. At this energy the conversion cross section $\sigma(\Sigma N \to \Lambda N)$ is rather small. This explains why the primordial Σ's do not transform easily. Furthermore, if they do, they generate highly energetic Λ's which are not good candidates for capture. Therefore, Σ-hypernuclei are more easily made (and by primordial Σ's) in $B=1$ annihilations compared to $B=0$ ones. If we combine the results of this section with those of sect. 4, we can write the total yield as

$$H = P_0 H_0 + P_1 H_1 , \tag{7.6}$$

where P_0 and P_1 are the probabilities for having $B=0$ and $B=1$ annihilations, respectively. The yields, assuming $P_1 = 10\%$ or 20%, are given in table 3. With 10% of $B=1$ annihilation, one obtains a total yield in the U case of $\sim 5.3 \times 10^{-4}$ (using the intermediate value of E_{PF}), which is close to the experimental value. Due to the uncertainties of the calculation, one cannot however conclude that $B=1$ annihila-

TABLE 3

Theoretical predictions for hypernucleus formation assuming 10% and 20% of $B=1$ annihilations

	^{209}Bi			^{238}U		
	$E_{PF}=40$	$E_{PF}=50$	$E_{PF}=60$	$E_{PF}=10$	$E_{PF}=15$	$E_{PF}=20$
$P_1=0.10$	18.37	23.33	29.12	3.53	5.27	7.41
$P_1=0.20$	26.12	32.41	39.76	4.90	7.49	10.52
exp. [12])		8-40			6.5 ± 2	

E_{PF} is given in MeV, yields in 10^{-4}.

tions are necessary to explain the results of PS177. But, they cannot be excluded either. More quantitatively, one may state that they are presumably excluded with a rate larger than ~20%.

We have checked that $B = 1$ annihilations do not modify the trend observed in fig. 6 for the angular correlation between the kaon and the hypernucleus.

8. Conclusion

We have studied here, by an elaborate INC model, the formation of hypernucleus after antiproton annihilation on nuclei, enlarging the basic scenario proposed by the PS177 collaboration. We pointed out that the whole process is rather complex, involving several contributions to the hypernucleus yield. We especially underlined the role of the excitation of the target remnant for limiting the detectability of the hypernucleus in the delayed fission channel. We have also shown that, due to the complexity of the excitation–deexcitation process, the predicted yields (of our calculation and of similar ones) cannot be taken more seriously than within a factor of 2 or so. In view of this uncertainty, one cannot state that the observed hypernucleus yield is inconsistent with the conventional picture of an antiproton annihilating on a single nucleon with subsequent rescattering. Room is still left for annihilation on two nucleons. Semi-quantitatively, our calculation yields an upper limit of the frequency of this process around ~20%.

Our model does not exhaust all possible manners to generate hypernuclei. The η-mesons issued from the annihilation can create a hyperon ($\eta N \to YK$), but the yield is negligible at low energy. We also neglected associated production through the $\pi N \to YK$ reaction, for the same reasons. The case of the $\bar{K}^*$'s is less trivial since they are produced in the annihilation quite abundantly ($\langle \bar{K}^* \rangle \approx \frac{1}{3}\langle \bar{K} \rangle$), but a large part of them will decay in a $\bar{K}$-meson before interacting with the nuclear medium. It is hard to estimate the qualitative effect of the introduction of $\bar{K}^*$. Their interaction cross section is presumably larger than for $\bar{K}$'s, but when they decay, they produce highly energetic antikaons, outside the magic kinematics. In any case, the net effect is certainly smaller than ~10%.

We disregarded the quantum effects of the hyperon capture. As we have said in sect. 5, these effects are presumably very much dilute by the summation over many final states. Furthermore, the quantum treatment [32]) precludes the treatment of the excitation by all the cascading particles in a consistent manner. Finally, it is limited to simple one-particle-one-hole configurations. The comparison of our treatment with the quantum approach of ref. [32]), although being not obvious for reasons mentioned in sect. 5.2, indicates that the uncertainty due to neglecting quantum effects is certainly smaller than the one linked to the description of the excitation process.

We emphasize the smallness of the factor $P(E^* < E_{PF})$, see eq. (3.7b). This means that a large number of the hypernuclei produced by annihilation products undergo

prompt fission. This point should be kept in mind for future studies in heavy hypernucleus physics.

Concerning the general problem of the search for $B=1$ annihilations, clear indications exist for deuteron targets only, namely the existence of the $\bar{p}d \to p\pi^-$ process [35]) and the large momentum tail in the proton spectrum both in strange [36]) and non-strange channels [37]). The latter point is critically examined in ref. [38]) and substantiated by the detailed theoretical investigation of ref. [39]). The experiments measuring the Λ and K_S yields in heavy targets have been shown to be consistent with the conventional picture [6-8]). At least, they do not show strongly enhanced strangeness production and in one case [10]), a suppression seems to exist. The nature and the spectrum of the cascading particles being different in $B=0$ and $B=1$ annihilations, it might very well happen that there too, room is left for $B=1$ annihilations, with some limited rate, of course. This point has not been investigated so far. Therefore, even in these cases, as well as in the problem considered in this paper, the $B=1$ annihilation process has not been disproved.

The hypernuclear hypothesis for delayed fission has not been clearly demonstrated and the correlation study of ref. [34]), even reexamined in the light of our results, is still inconclusive although it admittedly sheds some doubt about the validity of the hypothesis. Further measurements are needed, as well as a more systematic study on various targets. Highly fissile targets should be considered, in order to avoid the problem of the relationship between the hypernucleus yield and the prompt fission yield. From the theoretical point of view, calculations should be refined, especially in their description of the deexcitation process.

We are very grateful to Drs. M. Rey-Campagnolle, G.A. Smith and J. Žofka for stimulating discussions.

Note added in proof: We have been informed recently by the members of the PS177 collaboration that the results of the experiment on the kaon-hypernucleus correlation, mentioned in sect. 6.2 and cited in ref. [3]), should be considered as preliminary and are being reanalyzed. Therefore, our results contained in part (a) of fig. 6 should be considered as a prediction for the time being and the conclusion at the end of sect. 6 as premature. We are grateful to Dr. M. Rey-Campagnolle for an interesting correspondence on this point.

References

1) J.-P. Bocquet *et al.*, Phys. Lett. **B182** (1986) 146
2) J.-P. Bocquet *et al.*, Phys. Lett. **B192** (1987) 312
3) M. Rey-Campagnolle, preprint CERN-EP/89-124
4) J. Rafelski, Phys. Lett. **B207** (1988) 371
5) J. Cugnon and J. Vandermeulen, Phys. Lett. **B146** (1984) 16

6) C.B. Dover and P. Koch, invited talk at the Conference on Hadronic Matter in Collision, Tucson, Arizona, Oct. 88 and preprint BNL-42105
7) J. Cugnon, P. Deneye and J. Vandermeulen, Phys. Rev. C, in print
8) W.R. Gibbs and J.W. Kruk, Phys. Lett. **B237** (1990) 317
9) K. Miyano *et al.*, Phys. Rev. **C38** (1988) 2788
10) F. Balestra *et al.*, Phys. Lett. **B194** (1987) 192
11) G.T. Condo *et al.*, Phys. Rev. **C29** (1984) 1531
12) M. Rey-Campagnolle, Il Nuovo Cim. **A102** (1989) 653
13) P. Grangé, J.Q. Li and H.A. Weidenmüller, Phys. Rev. **C27** (1983) 2063
14) F. Scheuter, C. Grégoire, H. Hofman and J.R. Nix, Phys. Lett. **B149** (1984) 303
15) J.R. Nix, A.J. Sierk, H. Hofmann, F. Scheuter and D. Vautherin, Nucl. Phys. **A424** (1984) 239
16) P. Grangé, S. Hassani, H.A. Weidenmüller, A. Gavron, J.R. Nix and A.J. Sierk, Phys. Rev. **C34** (1986) 206
17) H. Poth, invited talk at the Workshop on Antimatter Physics at Low Energies, Batavia, Illinois, U.S.A., April 1986 and CERN-EP/86-105 preprint
18) J. Cugnon, P. Deneye and J. Vandermeulen, Nucl. Phys. **A500** (1989) 701
19) D.J. Millener, C.B. Dover and A. Gal, Phys. Rev. **C38** (1988) 2700
20) J. Cugnon and J. Vandermeulen, Phys. Rev. **C39** (1989) 181
21) G. Levman *et al.*, Phys. Rev. **D21** (1980) 1
22) J. Cugnon, P Deneye and J. Vandermeulen, Phys. Rev. **C40** (1989) 1822
23) W. Feller, An introduction to probability theory and its applications (Wiley, New York, 1957)
24) R. Vandenbosh and J.R. Huizenga, Nuclear fission (Academic Press, New York, 1973)
25) A. Gavron, H.C. Britt, E. Konecny, J. Weber and J.B. Wihelmy, Phys. Rev. **C13** (1976) 2374
26) J.R. Huizenga, R. Chaudhry and R. Vandenbosch, Phys. Rev. **126** (1962) 210
27) J. Cugnon, in The elementary structure of matter, ed. J.-M. Richard *et al.* (Springer, Berlin, 1980) p. 211
28) K. Killian, Proc. Workshop on nuclear physics with stored, cooled beams (McCormick's Creek State Park, Spencer, Indiana, AIP Conf. Proc. No. 128, ed. P. Schuandt and H.-O. Meyer (AIP, New York, 1984)
29) P. Jasselette, J. Cugnon and J. Vandermeulen, Nucl. Phys. **A484** (1988) 542
30) R. Armenteros and B. French, in High energy physics, ed. E.H.S. Burhop (Academic, New York, 1969). See also CERN proposal P28, 1980 (unpublished)
31) J. Cugnon and J. Vandermeulen, Ann. de Phys. **14** (1989) 49
32) H. Bandō and J. Žofka, Phys. Lett. **B241** (1990) 7
33) J. Žofka, private communication
34) T.A. Armstrong *et al.*, PS177 collaboration, to be published
35) R. Bizarri *et al.*, Lett. Nuovo Cim. **2** (1969) 431
36) B.Y. Oh *et al.*, Nucl. Phys. **B51** (1973) 57
37) J. Riedelberger *et al.*, Phys. Rev., to be published
38) V.M. Kolybasov, I.S. Shapiro and Yu. N. Sokolskikh, Phys. Lett. **B222** (1989) 145
39) M. Locher, Int. Conf. on medium- and high-energy physics, Taipei, ROC (1988)